Relative Mission Analysis for Proba 3: Safe orbits and CAM

T. V. Peters[(1)], D. Escorial[(2)]
[(1)(2)]GMV, C Isaac Newton 11, 28760 Tres Cantos, Spain, tpeters@gmv.com

Abstract: *This paper reports the phase B mission analysis work performed for the safe orbit and the Collision Avoidance Maneuvers (CAM) of the PROBA-3 formation flying mission, including the recovery to nominal conditions. PROBA-3 will perform formation flying in a highly elliptical orbit, and perform Solar coronagraphy and formation maneuvering demonstrations in a six-hour arc around apogee. Mission analysis in this paper addresses the safe orbit and the CAM and focuses on safety and ΔV requirements. Important constraints on the mission analysis are the absence of an omnidirectional sensor, and the requirement that the spacecraft cannot turn more than 30° away from the Sun due to thermal and power constraints. In addition, no on-board action can be taken after safe orbit entry nor after a CAM, which means that the recovery needs to be performed under ground control.*

Keywords: *PROBA-3, formation flying, mission analysis, safe orbit, CAM.*

1. Introduction

The PROBA-3 mission is designed to perform formation flying in a highly elliptical orbit. The formation consists of a coronagraph spacecraft (CSC) and an occulter spacecraft (OSC). The spacecraft are equipped with the following relative state sensors: both spacecraft are equipped with a GPS receiver and an inter-satellite link such that rGPS measurements can be made. The CSC is equipped with a Coarse Lateral Sensor (CLS) with a field of view of 5° and a Fine Lateral and Longitudinal Sensor (FLLS) with a field of view of 33 mm diameter at aperture. The spacecraft should not turn more than 30° away from the Sun direction due to thermal and power constraints. This limits the availability of the CLS and the FLLS to periods during which the angle between the CSC - OSC direction and the Sun direction is smaller than 30°. Figure 1 shows the Proba-3 spacecraft. The CSC is shown on the left and the OSC on the right.

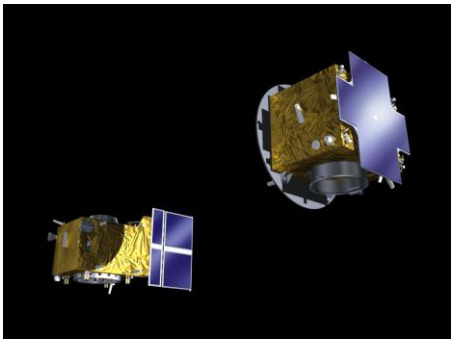

Figure 1. PROBA-3 Spacecraft

Orbital parameters of the reference orbit are shown in table 1. For simulations of transfer maneuvers the orbital parameters are assumed to be fixed, and the motion is assumed to be Keplerian. For simulations to determine the stability of the safe orbit, perturbations are taken into account for calculation of both the reference orbit and the relative orbit.

Table 1. Orbital parameters

Parameter	Value
Semi-major axis	36943 km
Eccentricity	0.8111 -
Inclination	59°
RAAN	84°
AoP	188°
Orbital period	19h38m

Table 2 presents the characteristics of the two spacecraft. Both spacecraft are equipped with a propulsion system. The CSC is equipped with a high-performance green propellant (HPGP) propulsion system with a thrust of 1 N, and the OSC is equipped a 10 mN cold gas system. The table also shows the parameters used for computing the solar radiation pressure (SRP) perturbation.

Table 2. Spacecraft characteristics

Parameter	OSC	CSC
Area [m2]	1.77	3.34
Wet mass [kg]	211	339
Dry mass [kg]	190	327
SRP coefficient [-]	1.9	1.29
Thrust per thruster [mN]	10	1000
Number of thrusters in direction of minimum thrust [-]	1.43	2.1
Fraction of thrust allocated for control	0.2	-

Table 3 lists the accuracy of the relative navigation. In addition to sensors listed in the table the CSC is equipped with a Coarse Lateral Sensor (CLS). This sensor is used during the process of acquisition of the FLLS, such that only the FLLS-based relative navigation is used for computing maneuvers. For this reason the CLS is omitted.

Table 3. Relative navigation accuracy

Parameter	Relative GPS	FLLS
1σ position bias [cm]	4.07	-
1σ velocity bias [mm/s]	0.0160	-
1σ position error [cm]	2.05	0.3
1σ velocity error [mm/s]	0.0228	0.005
1σ position bias [cm]	4.07	-

GPS measurements are available in the region around perigee. The values presented in the table for the accuracy of the relative GPS solution are valid for the moment the formation exits the GPS visibility region. From that point onward, the accuracy degrades because the solution needs to be propagated. FLLS measurements are available whenever the two spacecraft are properly aligned.
This paper describes the mission analysis work performed for the off-nominal conditions, the safe orbit and the collision avoidance maneuvers (CAM). The mission analysis work for the nominal operations is described in [1].

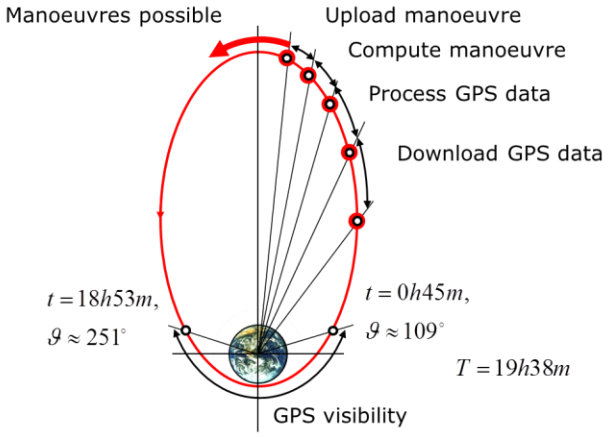

Figure 2. Ground control maneuver upload sequence

Recovery from all off-nominal conditions is performed under ground supervision. This means that the ground needs to take the steps described in figure 2 before each maneuver is performed. First the navigation data needs to be downloaded. Next a relative navigation solution needs to be obtained. Finally, the maneuver needs to be computed and uploaded to the spacecraft. In investigation of the ground contacts with Redu has shown that a maneuver at 160° true anomaly is possible during some orbits, but not all. On the other hand, the errors associated with the GPS measurements start increasing rapidly after passing apogee. Simulations have shown that maneuvers under ground control should be performed no later than 190° true anomaly. Under these restrictions gaps of up to 2 orbits exist between periods during which the ground control maneuver upload sequence shown in figure 2 can be used.
Two reference frames are used in the analysis of the relative motion. These are the LVLH frame and the VBAR frame. For both frames, the y-axis points into the direction of the negative orbital angular momentum vector. The z-axis of the LVLH frame points in the direction of the center of the Earth and the x-axis completes the right-handed frame. The VBAR frame uses a different definition. The x-axis points in the direction of the orbital velocity vector and the z-axis completes the right-handed frame.
The structure of the paper is as follows. The safe orbit is discussed first. The safe orbit is first defined in terms of its Cartesian state. Next, the stability and the sizing of the safe orbit are discussed. Finally, all maneuvers related to the safe orbit are investigated. These are, the entry into safe orbit, resizing of the safe orbit and return from safe orbit to nominal conditions. The CAM is discussed in the third chapter. The stop distance is discussed first, followed by a detailed description of the CAM algorithm. The behavior

over comparatively short timescales is investigated, and the return to mission is discussed. Finally, the long term behavior is investigated.

2. Safe orbit

The safe orbit is a stable non-drifting close formation flying trajectory that can be used for storing the formation during the long-eclipse season when eclipses occur around apogee for about 15 days, or after a minor malfunction has taken place and ground intervention is required. It is also used during the initial deployment and commissioning of the formation (see also [1]).

2.1. Overview

The safe orbit is designed as a generalization of the eccentricity / inclination vector separation strategy that is used for formation flying in circular orbits. The safe orbit is defined in terms of the differential eccentricity and angular momentum vectors, in such a way that the coronagraph spacecraft is above or below the occulter spacecraft at apogee and perigee. The differential angular momentum vector is perpendicular to the differential eccentricity vector, such that the resulting trajectory never intersects V-bar.

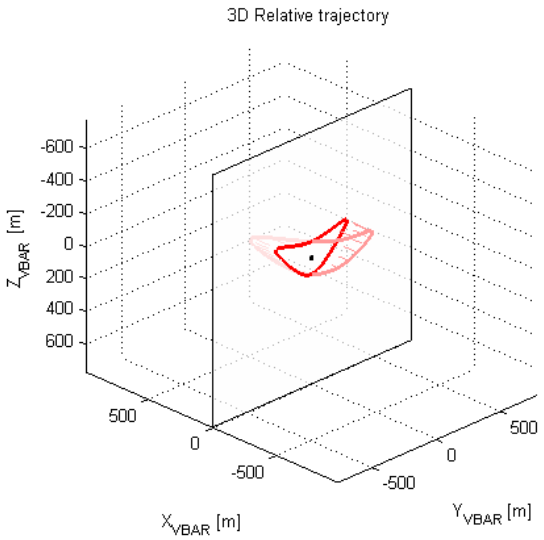

Figure 3. Safe Orbit

Figure 3 shows the safe orbit trajectory. Representation of the trajectory in the V-bar aligned reference frame is advantageous because in this frame the projection of the trajectory on the YZ-plane is independent of the along-track coordinate [2]. The safety of a trajectory can be determined by inspecting the closest approach of the trajectory in the YZ-plane. The safe orbit can be defined in terms of a Cartesian state vector in the LVLH reference frame.

$$\mathbf{x}_{safe,ip} = \pm D\rho^{-1}\left[-(1+\rho)\sin\vartheta \quad -c \quad -\left(\rho^{-2}(e\rho+c)+c\right)k^2\rho^2 \quad sk^2\rho^2\right]^T$$
$$\mathbf{x}_{safe,op} = \pm D\left(1+e^2\right)\rho^{-1}\left[\sin\vartheta \quad \rho^{-1}(\cos\vartheta+e)k^2\rho^2\right]^T \tag{1}$$

Where:

D is the characteristic dimension of the formation,
a is the semi-major axis of the reference orbit,
e is the eccentricity of the reference orbit,
$k^2 = \sqrt{\mu p^{-3}}$, $\rho = 1 + e\cos\vartheta$, $p = a\left(1-e^2\right)$, $s = \rho\sin\vartheta$, $c = \rho\cos\vartheta$
ϑ is the true anomaly of the reference orbit,
μ is the gravitational parameter

Four configurations are possible for the safe orbit, depending on the sign of the in-plane and out-of-plane motions. The first configuration has positive sign for both in-plane and out-of-plane motion, the second has negative sign for in-plane and positive sign for out-of-plane motion, the third has positive sign for in-plane and negative sign for out-of-plane motion and the fourth has negative sign for both in-plane and out-of-plane motion.

2.2. Safe orbit stability

The stability of the safe orbit is analyzed for various dates by propagating the orbits of the OSC and the CSC using an absolute propagator for both and subtracting the results. The reference orbit is taken as initial conditions for generating the orbit of the OSC. The initial conditions for generating the orbit of the CSC are obtained as follows. First, the Cartesian LVLH state vector is converted to differential orbital elements by means of a linear transformation [3]. Next, the linear differences in orbital elements are added to the orbital elements of the reference orbit.

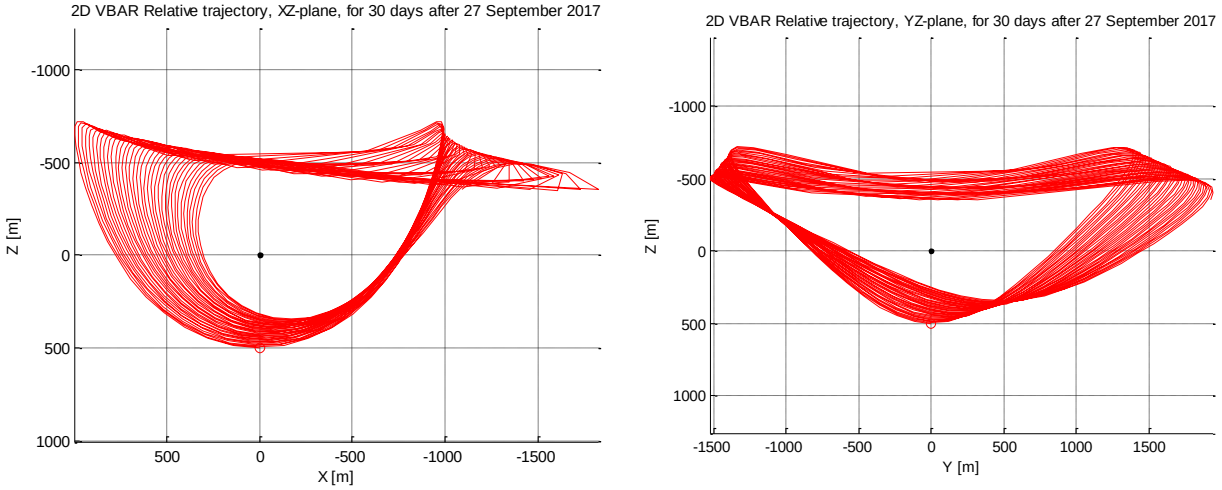

Figure 4. Safe orbit stability for 30 days, XZ (left) and YZ (right) projection (left)

The first year has been divided into 12 segments, and long term simulations have been performed for each. Figure 4 shows the worst case evolution of the safe orbit during a 30 day propagation period. SRP has the largest perturbative influence, followed by J2. Figure 5 shows the evolution of the inter-satellite distance (ISD). The minimum ISD decreases to 290 m after 30 days. This figure confirms that the safe orbit is indeed safe for 30 days.

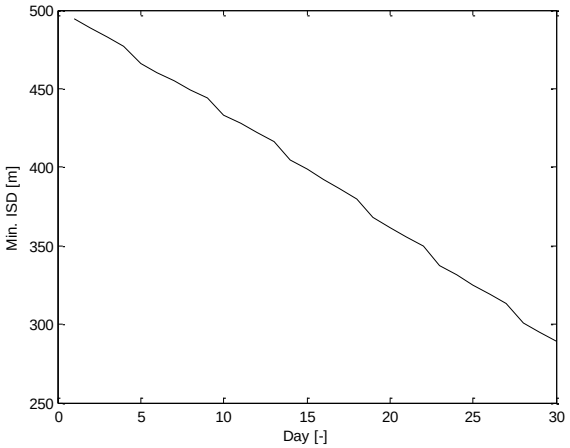

Figure 5. Worst case evolution of ISD

Substantial along-track drift may also be present when the safe orbit is initialized. This drift has two main causes, namely, dispersions caused by navigation and actuation errors during safe orbit entry and unmodelled J_2 effect. The J_2 effect is important if transfer starts close to perigee. The cause of this phenomenon is that the J_2 perturbation causes short-period oscillations in the semi-major axis (and the other elements, but the effect is less important) which the unperturbed, linear guidance model does not take into account. Both effects can lead to an along-track drift of about 13 km in 30 days, summing to a total of 26 km in 30 days.

2.3. Safe orbit sizing

The sizing of the safe orbit takes into account the stay time in the safe orbit, the insertion accuracy and the minimum approach distance.
The characteristic dimension of the safe orbit should be set large enough to be able to cope with safe orbit insertion uncertainties and the influence of perturbations, mainly J2 and SRP. The minimum characteristic dimension is determined as the sum of three contributions, namely, the maximum expected trajectory uncertainties at the point of closest approach, the maximum expected impact of the perturbations and the minimum ISD.
The stay time in the safe orbit determines the effect of perturbations on the trajectory; the longer the formation remains in safe orbit, the larger the effect of perturbations and the larger the safe orbit must be to accommodate perturbations. The insertion accuracy is determined by the navigation and the actuation accuracy. The actuation accuracy depends (amongst others) on the magnitude of the ΔV to be supplied, which in turn depends on the size of the safe orbit.

Table 4 reports the safe orbit options that lead to a safe transfer and a safe stay time for the specified period. It also shows the margins required to accommodate the perturbations and the dispersions associated with the transfer to safe orbit.
For the long eclipse season, a 15-day safety interval is required. In this case, the cumulative effect of perturbations is smaller than expected in section 2.2: the minimum ISD shrinks by about 100 m under the influence of J_2 and SRP. A margin of 100 m is therefore required to accommodate perturbations. The transfer itself has an insertion accuracy of 100 m. The minimum ISD has been chosen as 80 m for all safe orbit options, such that for a 15 day stay time a safe orbit with a characteristic dimension of at least 280 m is required. To make the safe orbit selection independent of the required stay time a characteristic dimension of 500 m is selected for the safe orbit regardless of the stay time. This leads to a simpler and more robust algorithm for selecting the safe orbit.

Table 4. Safe orbit sizing table

Duration (days)	perturbation margin (m)	insertion accuracy margin (m)	minimum ISD (m)	characteristic dimension (m)	min entry ΔV (mm/s)	max entry ΔV (mm/s)	ΔV to resize to 150 m safe (mm/s)
10	70	90	80	240	36	70	18
15	100	100	80	280	44	78	26
20	140	130	80	350	56	93	40
25	180	160	80	420	69	108	54
30	220	200	80	500	80	125	70

2.4. Safe orbit entry

The safe orbit entry has been investigated by means of extensive simulations. The transfer to safe orbit needs to be available for any orbit during the mission life and for any point along the orbit. The transfers have been investigated systematically, from a point along the nominal orbit sequence to each of the four configurations dividing each orbit into 20 steps of equal true anomaly during each orbit and for every date found by dividing the year in 10 steps during the first year (i.e., one transfer computed every 36 days). The transfer to a safe orbit of 500 m can always be performed safely. The maximum 3σ trajectory bounds due to insertion errors that can reasonably be expected are 190 m. The ΔV required to enter safe orbit from the nominal orbit routine lies between 80 and 125 mm/s.
Figure 6 shows an example of a transfer to safe orbit from nominal conditions with worst case actuation errors. Worst case trajectory uncertainties are associated with transfers to safe orbit that start in a region close to perigee. Within the set of cases that was investigated, the largest trajectory uncertainties at apogee or perigee always occurred for trajectories started within 70° of perigee.

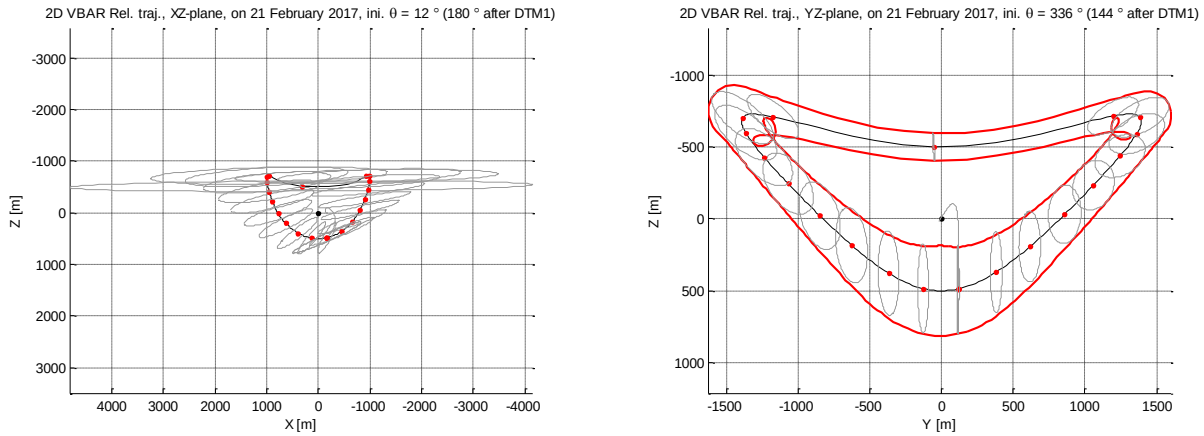

Figure 6. Transfer to safe orbit, worst case actuation errors

2.5. Resizing the safe orbit

In certain situations it is required to resize the safe orbit. To increase the stay time, for example, it may be required to enlarge the safe orbit. For returning from the safe orbit to nominal conditions it is required to shrink the safe orbit. Shrinking the safe orbit is the critical case, because dispersions due to actuation errors may cause the trajectory to become unsafe. Resizing the safe orbit is performed using a two-point transfer from a predetermined initial true anomaly to a final true anomaly that is chosen such that the total ΔV is minimized.

Two characteristic dimensions are used for the safe orbit, namely 500 m and 1000 m. A characteristic dimension of 500 m is used for brief mission interruptions, for example during long eclipse season. A characteristic dimension of 1000 m is used during the initial deployment and during the recovery from CAM maneuvers. Dispersions due to actuation errors prevent a direct transfer from a safe orbit to nominal conditions if the characteristic dimension of the safe orbit is larger than 200 m. This means that the safe orbit needs to be shrunk before the return to nominal conditions can be performed. Dispersions due to actuation errors limit the extent to which the safe orbit can be shrunk in a single step. The safe orbit can be safely shrunk to a characteristic dimension of 150 m from an initial characteristic dimension of 500 m. If the initial characteristic dimension is 1000 m, then the safe orbit should first be shrunk to a characteristic dimension of 250 m.

Figure 7 shows an example of a shrinking operation from a characteristic dimension of 1000 m down to a characteristic dimension of 250 m. The initial conditions for the shrinking operation are representative of the safe orbit at the end of formation deployment and the CAM recovery, including dispersions. The transfer takes place from a true anomaly of 160° to a true anomaly that minimizes the transfer ΔV. This true anomaly lies between 180° and 195°. Figure 7 shows the initial and final safe orbit during the shrinking operation. In this example, the ΔV required for shrinking the safe orbit is 145.31 mm/s, with a 3σ uncertainty of 13.75 mm/s.

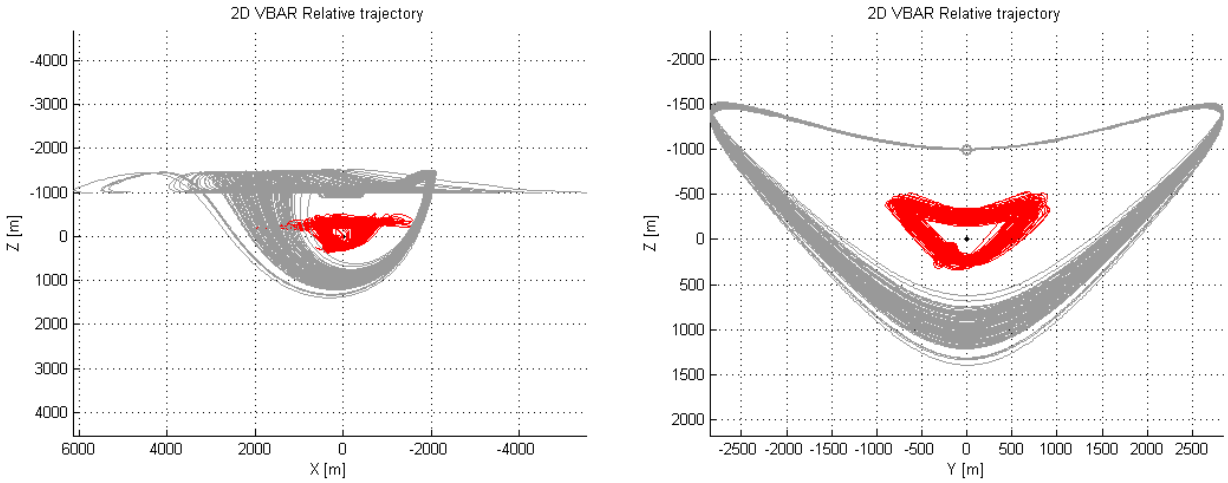

Figure 7. Shrinking the safe orbit from 1000 m to 250 m

2.6. Return to nominal conditions

The strategy for returning to nominal operations depends on the time the spacecraft have spent in safe orbit. Safe orbit is not controlled, so, the longer the spacecraft remain in safe orbit, the longer perturbations will act on the trajectory and cause dispersions. The analysis in the previous paragraph has shown that the trajectory can drift over quite a large along-track distance, and that it can be deformed quite a lot during 30 days. It is therefore quite likely that the safe orbit trajectory will first need to be corrected. It is assumed that the process to correct the trajectory ends in a safe orbit with accuracy determined by the navigation and actuator accuracy.

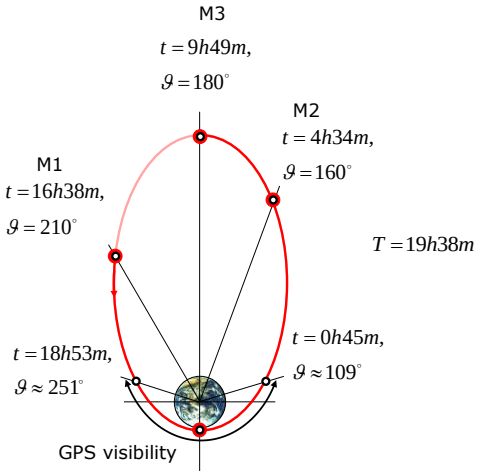

Figure 8. Transfer from safe orbit to nominal conditions

The return from the safe orbit to nominal orbit conditions is examined to ensure that the OSC is in the field of view of the CLS at the end of the transfer to the nominal orbit. This condition needs to be satisfied such that the on-board formation flying software can

successfully take over at that point. All maneuvers up to this handover are performed under ground command. Figure 8 shows the maneuvering strategy for all maneuvers up to the handover point. The transfer is initiated as a two point transfer between a true anomaly of 210° to apogee of the next orbit. GPS measurements are taken when the formation passes through perigee and a correction maneuver is computed and uploaded before the formation reaches a true anomaly of 160°. The correction maneuver is a two-point transfer between a true anomaly of 160° and apogee.

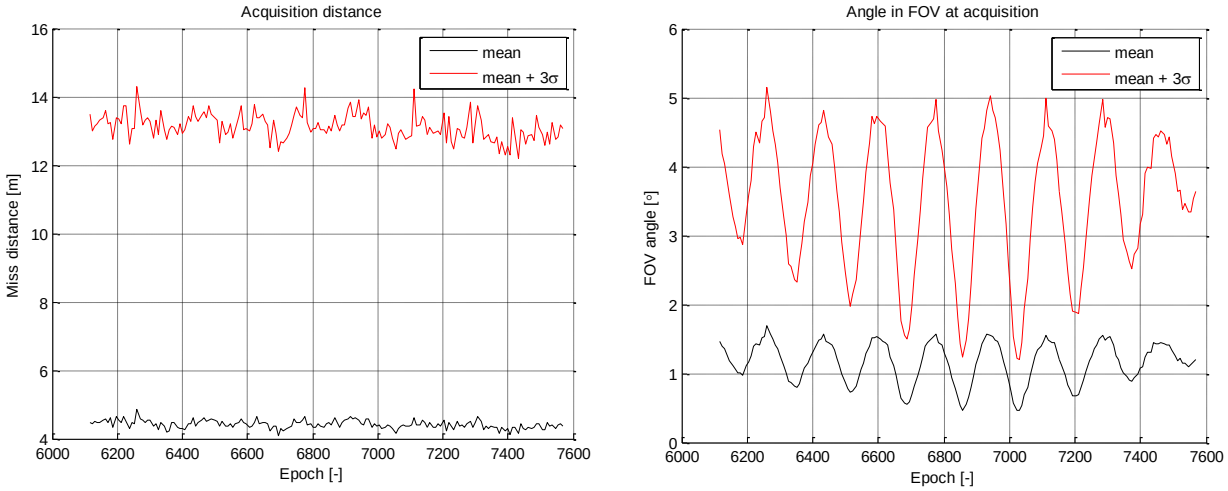

Figure 9. Miss distance (l); angle betw. CSC OSC direction and CLS bore sight (r)

Figure 9 shows the miss distance and the ISD at the terminal point. The mean approach distance is about 4.5 meters, while the mean + 3σ approach distance is about 13 meters. A related measure is the angle in the FOV at the terminal point. More precisely, this is the angle between the CSC-OSC direction and the CLS bore sight. It is calculated as the angle between the desired and actual terminal relative position vector: it is assumed that the CLS is pointed along the expected direction to the OSC, which is equal to the unit vector along the desired relative position vector of the OSC.
Figure 9 also shows the FOV angle. The mean + 3σ angle remains below 5° nearly all the time, although there are some dates (notably around 6250) at which the mean + 3σ angle is equal or slightly larger than 5°. The mean FOV angle fluctuates around 1°. The chances of finding the OSC in the CLS FOV after the transfer are quite high. The seasonally averaged, mean ΔV required for the impulsive transfer is 35 mm/s, and the mean + 3σ ΔV is 45 mm/s. On top of this a ΔV of 11.5 mm/s is required for the forced motion acquisition.

3. CAM

The CAM needs to provide active protection against collisions during a 10 hour arc around apogee. Both the OSC and the CSC need to be capable of providing the CAM. The CAM is designed based on considerations that cover the initial behavior during and right after the burn (the stop and departure), the behavior during the first few orbits and the long term evolution. These points can be summed up as follows:

1. Ensure that the spacecraft comes to a stop safely (if required)
2. Ensure that the spacecraft moves out safely
3. Ensure that the trajectory does not return to the origin
4. Ensure that no evaporation occurs

The CAM ΔV is computed as the sum of two contributions (applied as a single ΔV), namely, the ΔV required to stop the motion, and a ΔV that is required to put the spacecraft into a drifting trajectory with a specified drift distance. The second contribution is computed based on the drift distance and the current in-plane relative position vector. This section discusses the stop distance, the CAM algorithm, the short-term behavior after the CAM, the return to mission and the long-term behavior.

3.1. Stop distance

The CAM maneuver is applied when one spacecraft crosses the boundary of a stop sphere around the other spacecraft. The sizing of the stop sphere should be such that during the time between the start of the application of the CAM and the end of the application of the CAM, no collision can occur. The implication of such a strategy is that the size of the stop sphere is dependent on the maximum expected relative velocity of the formation, and on the minimum expected dimensions of the formation. The stop distance can be estimated by assuming that the spacecraft are moving in gravity-free space and that the spacecraft performing the CAM thrusts continuously in the direction opposite to the relative velocity until the motion is stopped. Under these assumptions the stop distance is given by:

$$d = \tfrac{1}{2}\left(\frac{m}{F}\right)V^2 \tag{2}$$

The OSC is equipped with cold gas thrusters, such that the CAM performed by the OSC is the critical case for determining the stop distance. Simulations have shown [1] that the maximum velocity in the 10 hour region around apogee is 20 mm/s for the nominal orbit. This leads to a stop distance of about 7 m for the OSC. This value for the stop distance is compatible with the minimum ISD during formation flying of 25 m.

3.2. CAM algorithm

The algorithm computes the ΔV as the sum of two components, ΔV_1 and ΔV_2.

$$\mathbf{\Delta V}_{CAM} = \mathbf{\Delta V}_1 + \mathbf{\Delta V}_2 \tag{3}$$

The first component nullifies the velocity. The y-component of the velocity is only nullified if it is directed towards the target.

$$\mathbf{\Delta V}_{1,ip} = -\begin{bmatrix} v_{x,LVLH} \\ v_{z,LVLH} \end{bmatrix}, \qquad \Delta V_{1,op} = \begin{cases} 0 & \operatorname{sgn}\left(v_{y,LVLH}\right) = \operatorname{sgn}\left(y_{LVLH}\right) \\ -v_{y,LVLH} & \operatorname{sgn}\left(v_{y,LVLH}\right) \neq \operatorname{sgn}\left(y_{LVLH}\right) \end{cases} \tag{4}$$

Where:

$v_{x,LVLH}, v_{y,LVLH}, v_{z,LVLH}$ Cartesian velocity vector components in the LVLH frame.

The second component of the ΔV is to be applied along V-bar. The magnitude of ΔV_2 can be computed from the current x and z components of the position vector and the desired drift rate per orbit:

$$\Delta V_2 = \frac{k^2 a \eta^4}{2\sqrt{2\rho - \eta^2}} \left(\mp \frac{\eta}{3\pi a (1-e)} D_{des} + \frac{2\rho^2}{a\eta^4} \left(e \sin \vartheta \cdot x_{LVLH} + (1+\rho) z_{LVLH} \right) \right) \quad (5)$$

Where:

$\rho = 1 + e\cos\vartheta$, $\eta = \sqrt{1-e^2}$, $k^2 = \sqrt{\mu p^{-3}}$, $p = a\eta^2$,
a is the semi-major axis of the reference orbit,
e is the eccentricity of the reference orbit,
D_{des} is the desired drift rate per orbit.
ϑ is the true anomaly of the reference orbit,
μ is the gravitational parameter,
x_{LVLH}, z_{LVLH} are the in-plane Cartesian position vector components in the LVLH frame.

The sign of the desired drift rate depends on the direction of the in-plane ΔV. The direction is chosen such that the initial velocity after the CAM is directed away from the origin. The second component of the ΔV is given by:

$$\mathbf{\Delta V}_{2,ip} = \Delta V_2 \cdot \frac{1}{\sqrt{2\rho - \eta^2}} \cdot \begin{bmatrix} \rho \\ e \sin \vartheta \end{bmatrix} \quad (6)$$

3.3. Short term behavior

The CAM algorithm has been simulated using Monte Carlo simulations. The initial position is randomly selected lying on a sphere with a radius of R. The initial velocity follows a Gaussian distribution on all components, such that the mean value takes on a particular value of 20 mm/s. The simulation uses a constant acceleration thrust arc in the VBAR reference frame to perform the CAM. An uncertainty of 5% in magnitude (1σ) and 1° in direction (1σ) is applied to the ΔV vector. After the thrust arc the trajectory is propagated for two full revolutions and the minimum ISD during the full trajectory is stored.
Three simulations are performed; one at close range, the second at medium range, and the third at a long range. Figure 10 shows the results of these simulations. The initial conditions for the short range simulation (left) lie on a sphere of radius 30 meters, with a mean velocity of 20 mm/s. The drift per orbit is set to 200 m. The initial conditions for the medium range simulation (middle) lie on a sphere of radius 75 meters, with a mean

velocity of 20 mm/s. The drift per orbit is set to 500 m. The initial conditions for the long-range simulation (right) lie on a sphere of radius 160 meters, with a mean velocity of 20 mm/s. The drift per orbit is set to 800 m.
The red points represent the results of the Monte Carlo simulations. The black lines represent a theoretical evaluation of the stop distance based on equation (2). The short term behavior of the CAM algorithm corresponds well with the expectations of the minimum approach distance described in section 3.2.

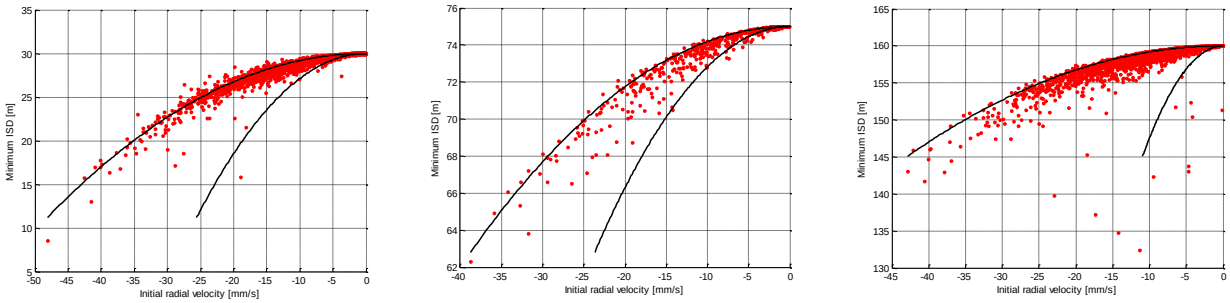

Figure 10. Minimum approach distance

3.4. Return to mission

The recovery strategy after a CAM maneuver is similar to the deployment of the formation. The recovery after CAM should be as rapid as possible not to lose operational time. The precision with which the spacecraft returns to the safe orbit around the origin should be high so the precision with which maneuvers are performed should be high as well. The absolute size of the error in the maneuver execution of the maneuvers depends on the size of the maneuver, such that ΔV's should be small during the approach strategy to achieve increased accuracy.

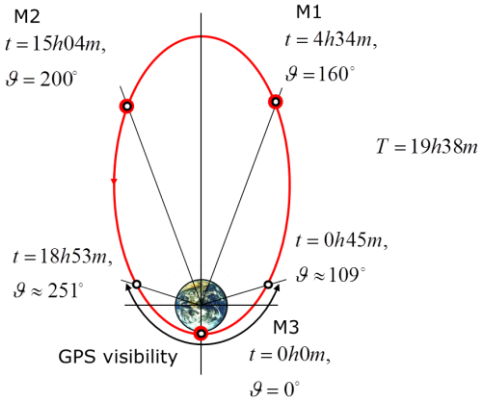

Figure 11. Maneuver location diagram for CAM recovery

Figure 11 shows the locations of the maneuvers with respect to the reference orbit. Maneuver 1 takes place at 160°, maneuver 2 takes place at 200° and maneuver 3 takes place at 0° true anomaly.
Figure 12 shows the CAM trajectory and the recovery after the CAM. The procedure followed to obtain this CAM recovery trajectory is based on ground computation of

maneuvers. The sequence of maneuvers is the following. During the first orbit, a two-point transfer to safe orbit is computed on-ground and uploaded to the spacecraft. The maneuver is computed and uploaded just before 160°, such that the first ΔV is performed at 160° and the second ΔV at the optimal point in orbit. These two maneuvers are point 1 and 2 in the figure.
During the second orbit, a three-burn transfer to make the safe orbit drift to the origin is computed and uploaded. The maneuver is computed and uploaded just before 160° such that the first ΔV is performed at 160°, the second ΔV is performed at 200°, and the third ΔV is performed at perigee. These three maneuvers are labeled 3, 4 and 5 in the figure. Note that a number of drifting orbits (and correction maneuvers) can be inserted between maneuvers 4 and 5. In this case, a single drifting orbit (orbit three) is inserted.
After maneuver 5 the spacecraft is in a safe orbit with characteristic dimension of 1000 m around the origin. During the fourth the safe orbit (not shown in the figure) is shrunk from 1000 m to 250 m (see section 2.5). During the fifth orbit (not shown in the figure) ground commands the sequence of maneuvers to return the spacecraft to nominal conditions as described in section 2.6.

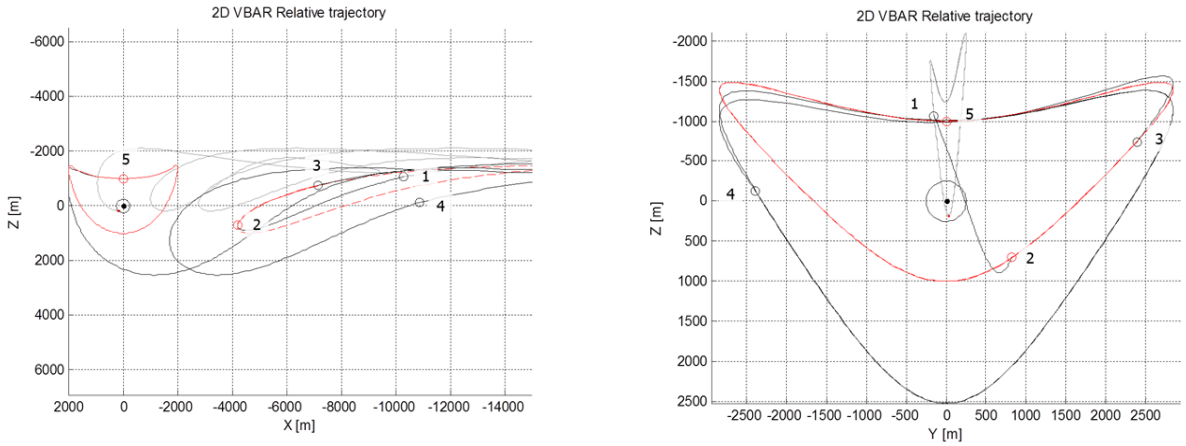

Figure 12. Ideal CAM recovery trajectory

The recovery trajectory is robust to the non-execution of any of the maneuvers, that is to say, the recovery trajectory is composed of passively safe trajectory elements [4]. The CAM and the recovery have been simulated using Monte Carlo simulations. These simulations have shown that the total impulsive ΔV required for the CAM and the recovery is 610 mm/s with a standard deviation of 73 mm/s. A ΔV of 11.5 mm/s is required for the forced motion acquisition at the end of the recovery.

3.5. Long term behavior

In case the drifting time after CAM is larger than 5 orbits, the strategy presented in section 3.4 will have to be complemented with a two point transfer maneuver to recover most of the drifting distance in a fast way before the return to nominal conditions defined above is started. A parametric analysis has been carried out on this maneuver taking into account the type of CAM performed, the drifting time and the recovery time. Both

mean and maximum ΔV has been computed through a Monte Carlo campaign of 10000 shots varying the initial position (on a sphere of radius R0) and the initial velocity (average velocity 20 mm/s).
Table 5 summarizes the required ΔV for the initial part of the recovery after a CAM. The ΔV has been computed in previous sections as a function of the type of CAM (short, medium, long), the drifting time after the CAM (60, 30 days) and the number of orbits in which the recovery to the intermediate point has to be performed (5.7, 2.7 and 0.7 orbits). For each case the mean ΔV and maximum ΔV is presented. As can be seen from the data, the longer the drifting time, the larger the distance to be recovered and the larger the required ΔV. On the other hand, the larger the allowed recovery time, the lower the ΔV.

Table 5. Recovery ΔV in m/s

Return in # orbits		5.7		2.7		0.7	
Drifting days		60	30	60	30	60	30
Short range	mean ΔV	0.770	0.449	1.407	0.659	2.428	1.049
	max ΔV	0.295	0.149	0.511	0.257	1.041	0.523
Med. range	mean ΔV	1.459	0.800	2.712	1.287	4.347	2.203
	max ΔV	0.739	0.372	1.279	0.647	2.612	1.308
Long range	mean ΔV	2.382	1.281	3.805	1.932	6.808	3.354
	max ΔV	1.176	0.595	2.044	1.030	4.189	2.093

4. Conclusions

This paper has shown that the strategies developed for all maneuvers related to the safe orbit and the collision avoidance maneuvers for PROBA-3 are feasible. All maneuvers are safe, and can be performed under ground control. Control can successfully be handed back to the spacecraft after ground commands a transfer from the safe orbit to nominal conditions

5. References

[1] Peters, T. V., Branco, J., Escorial, D., Tarabini Castellani, L. , Cropp, A., “Mission Analysis for Proba-3 Nominal Operations, ” IWSCFF-2013-07-06, Proceedings of the 7th International Workshop on Satellite Constellations and Formation Flying, 13 – 15 March 2013, Lisbon, Portugal
[2] Peters, T. V., Peyrard, J., Carrascosa, C., “Safe Trajectories for PROBA-3”, Proceedings of the 4th International Conference on Spacecraft Formation Flying Missions & Technologies, St-Hubert Quebec, 18 – 20 May 2011
[3] Schaub, H., Junkins, J.L., “Spacecraft Formation Flying,” Analytical Mechanics of Space Systems, AIAA, Reston VA, 2003, pp. 593-674, doi: 10.2514/4.861550
[4] Fehse, W., “Automated Rendezvous and Docking of Spacecraft”, 1st ed., Cambridge University Press, Cambridge (UK), 2003